

Study the Damage Effects of Different Laser Pulses on the Pyrotechnic Bridge

Junxia Cheng¹, Bo Tian², Kexin Han¹, Jiangxu Wang¹, Jia Wang¹, Dangjuan Li¹ and Shenjiang Wu¹

¹School of Photo-Electrical Engineering, Xi'an Technological University, Xi'an, 710021, China.

²College of Aerospace and Civil Engineering, Harbin Engineering University, Harbin, 150001, China.

*Corresponding author

Shenjiang Wu, School of Photo-Electrical Engineering, Xi'an Technological University, Xi'an 710021, China

Submitted: 22 Feb 2022; Accepted: 01 Mar 2022; Published: 17 Mar 2022

Citation: Junxia Cheng, Bo Tian, Kexin Han, Jiangxu Wang, Jia Wang, Dangjuan Li and Shenjiang Wu (2022) Study the Damage Effects of Different Laser Pulses on the Pyrotechnic Bridge. *J Pla Che Pla Pro Res*, 3(1): 07-14.

Abstract

Lasers are used more and more widely in daily life, medicine and aerospace fields, which promoted the development of all kinds of laser and laser technology. With the continuous breakthroughs in the research field, the application of high power lasers is also more extensive. When the frequency doubling light is emitted from the laser, different wavelengths will act on the separation film simultaneously. Therefore, it is necessary to investigate the damage of optical thin films by laser of single wavelength or multiple wavelengths. The film was irradiated repeatedly by laser aiming, and the damage radius and damage morphology were studied under the action of 1064nm laser and 532nm laser alone and together, as well as the primary and secondary relationship of the damage induced by the two wavelengths. Then, the distribution of explosive damage temperature field was analyzed by simulation. It is concluded that the damage radius at 532nm is larger than that at 1064nm, and the damage depth is deeper. When the two pulses work together, 532nm laser plays a dominant role in the damage process. This study is helpful to better understand the damage mechanism of bridge film and provide reference for the preparation of damage-resistant explosive bridge and laser ignition.

Keywords: Explosive Bridge; Laser Damage; Multi-Pulse; Temperature Field Distribution

1. Introduction

The elements of thin film are very important in laser system, but it's a vulnerable link. The damage caused by the interaction between laser and thin film has been the important reason, which restricts the development of laser towards higher power and higher energy. The bridge thin film of initiating explosive device is an important component of remote sensing satellite detection, but destruction of thin film device by high-intensity laser weapon can cause functional failure of satellite [1]. Therefore, it is of great practical significance to study the damage threshold of components and damage caused by different lasers in order to further improve the system and expand its application in scientific research and production. Laser damage to explosive bridge materials depends not only on material properties and laser properties, but also on the external environment factors. The sensitive impurities with different radii by the same wavelength laser are the main factors for damage and temperature rise. Material properties include optical, thermal and mechanical parameters such as optical transmittance, absorption coefficient, thermal conductivity and laser damage resistance. Laser characteristics include energy, wavelength, power, pulse width, pulse structure, and repetition rate, etc. [2]. Any of these factors can affect the laser damage process leading to a certain extent.

In recent years, some laboratories have carried out experiments on damage caused by lasers of two wavelengths together. For example, lasers are used to irradiate crystals for several times to study the radius growth coefficient of damage pits and damage morphology difference under single and joint action respectively [3]. proposed an impurity induced damage model used to analyze the thermal damage and stress damage of block materials caused by impurities [4]. Explored the influence of impurity absorption cross section, absorption depth and temperature on the damage [5]. Based on practical observation and theoretical analysis, the researchers analyzed the effects of various laser parameters on the damage of different optical glasses and thin films, who proposed the avalanche ionization, multi-photon ionization, self-focusing, defect and impurity damage mechanisms, and gave a preliminary theoretical explanation for these damages. Theoretically studied the damage of optical films, and analyzed the effects of laser wavelength, pulse width and film thickness on the damage threshold [6]. Meanwhile, they mad a comparison for the damage mechanisms such as avalanche damage, multi-photon absorption and impurity induction. Conducted numerical simulation of the damage process caused by impurities. In addition, the damage morphology and damage threshold of optical films irradiated by 1.06 μ m laser with different pulse widths and irradiation areas were tested by

European joint laboratories, which the effects of different experimental environments on the damage of optical films were obtained [7]. Established the standing wave field theory of multilayer films by combining Maxwell equations [8]. Analyzed the reasons of absorption damage at the interface of optical thin films through experiments, and gave the damage threshold of different structures (9, 10). Respectively explored real-time detection methods of thin film damage, such as the laser thermal deflection imaging method and reflection scanning method [11, 12]. Gave suggestions and schemes for laser pretreatment technology of thin films [13].

In this paper, the damage morphology and temperature field distribution of different laser energy on different materials are studied by experiment and simulation. Firstly, the damage threshold of explosive bridge was measured by 1064nm and 532nm single wavelength laser respectively, and the damage morphology of bridge film under different laser energies was compared and analyzed. Furthermore, COMSOL was used to simulate the single wavelength and dual wavelength to explore the damage of the explosive bridge film and obtain the time evolution of the temperature field under different laser energy densities. Finally, by analyzing the mechanism, the primary and secondary damage factors induced by different laser wavelengths were determined.

2. Theory and Method

2.1 Laser damage mechanism of explosive bridge

This paper chooses double layer structure, the first layer is metal, the second layer is non-metallic materials. Generally, the damage mechanism of metal materials is intrinsic absorption and thermal damage, while the damage mechanism of non-metal materials is electron avalanche ionization. Therefore, the damage mechanism of explosive bridge is analyzed from these two aspects.

2.1.1 Intrinsic absorption and thermal damage

Laser damage is the result of the interaction between laser and optical material, including photothermal, photoelectric, material characteristics, laser energy, linear absorption, plasma formation and other physical processes. The metal layer is mainly the internal absorption mechanism and thermal damage [14]. The most direct cause of damage caused by the interaction between laser and explosive bridge film is the internal absorption of optical materials. It is supposed that the absorption coefficient of the optical element is α , the incident laser energy is J_0 , and the light intensity through the thickness d is reduced to:

$$J = J_0 (1 - R) (1 - e^{-\alpha d})$$

where, R is the reflectivity of the optical material surface. If α is small, then:

$$J = J_0 (1 - R) \alpha d$$

We given that c is the molecular heat capacity of the optical material, ρ is the density of the optical material, M is the relative molecular weight, and S is the spot area. Thus, the temperature limit

of the surface layer caused by laser absorption is:

$$\Delta T \approx J_0 (1 - S) \alpha M / \rho c$$

Any optical material has its own maximum temperature. If the surface temperature of the optical element reaches the material limit temperature, the material will be damaged. So, the melting point of the material or the thermal stress damage limit may be this limit temperature. In addition, the intrinsic absorption on the surface of optical materials can be considered to be relatively uniform. Adsorption and structural dissimilation may produce additional surface absorption on the surface of the material, which makes the damage of the optical surface easier. But the mechanism is relatively more complex, and such absorption generally occurs at the laser damage of the metal.

2.1.2 Electron avalanche ionization

Hacker derived the electron avalanche model of optical materials from the early concept of DC electron breakdown [15]. Its process is: the electronic absorption laser energy can be affect conductivity, allowing it to accelerate if electrons and valence electrons in the wire and collision ionization leads to absorb more energy. Then, it can produce multiple electronic, these electronic will continue to repeat the above process. Finally, that leads to the formation of laser plasma in the local area of material, and the conductivity have risen sharply. After 30 seconds of plasma activity and subsequent laser radiation, the initial slight damage becomes macroscopic damage. The model of electron avalanche ionization initially consists of minority free electron. Because there are metal impurities, defects, impurity ions or electronic defects in the dielectric, the theory requires semi-quantitative treatment. The solution process is as follows: the electron density function and electron avalanche ionization rate in the material are obtained by solving the equation, then the theoretical laser damage threshold is obtained by using the critical conductivity electron density ($\approx 10^{18} \text{cm}^{-3}$). The expression of the electric field intensity threshold E_{th} for the damage of wide-band gap media is as follows:

$$E_{th}^2 = 6E_g m_e^2 c_s / k_b T e^2 (\omega^2 + E_g / m_e L_{ac}^2) \frac{1}{\ln(t_p / L\theta)}$$

in which m_e is the quality, E_g is materials band gap energy, c_s is the sound velocity in the samples, L is the number of regenerated electrons, k_b is the boltzmann constant, T is temperature, e is the electron charge, L_{ac} is electronic-phonon mean free path of the collision, t_p is laser pulse width, ω is frequency of laser beam, θ is the parameter related to material properties and electric field strength. This parameter has little influence on the damage behavior when the material properties change little. Then, the above formula can be written as an energy density expression:

$$J_{th} = 0.5 \varepsilon E_{th}^2 t_p \propto \frac{t_p}{\ln t_p}$$

in the formula, ε is the electron energy, c is the speed of light, and J_{th} is the critical energy density when damage occurs, that is, the energy damage threshold. By combing with Equation [3] and [4],

the relationship between laser damage threshold, laser pulse width and laser wavelength can be obtained. Generally, the laser pulse width is proportional to the laser damage threshold response, while the laser wavelength is inversely proportional to the laser damage threshold.

2.2 Observation and simulation of damage morphology

Damage morphology analysis includes damage area and damage depth, which can be amplified more than 100 times by electron microscope and profilometer. The electron microscope mainly observed the area and irregularity of the laser damage, while the profilometer mainly observed the depth of the damage. At the same time, COMSOL software is used to simulate real physical phenomena by solving single-field or multi-field differential equations. It is widely used in physical fields such as fluid motion, heat transfer, structural mechanics, electromagnetic analysis, etc., which required models were built with various predefined applications. The software definition model is flexible and can modify material properties, source terms and boundary conditions. The specific values can be constants, any variable functions, logical formulas, or even direct interpolation functions representing the measured data. We can select the physical fields what want and define the relationships between them.

3. The Analysis and Discussion of Results

3.1 Laser damage at different wavelengths

Firstly, it need to calibrate the 1064nm laser energy and trigger the

laser three times to test until there is no abnormality. After calibration, wipe the sample with absorbent cotton dipped in alcohol, then fix it on the bracket and put it into the detection system to test the material damage. For comparison, a large spot is damaged by a laser with a higher energy density, and then the damage threshold is tested around the spot. It is also convenient for subsequent profiler and microscope observation. First, it set the energy density after attenuation to 100mJ, and then adjust the coordinate to trigger the laser in the adjacent position in turn.

According to the testing process, it is estimated that the laser damage energy of the sample is about 5mJ. After setting the energy of attenuation to 5mJ, a small but visible white spot was found on the surface when the laser was triggered. Generally, the laser damage threshold test needs to be evaluated at the critical point of the laser damage. But the above data cannot indicate that the energy 5mJ is the critical value of the damage energy density, so it needs to be verified. When the energy density is reduced to 2mJ, the damage is almost invisible in real time imaging. When the laser energy density was increased to 4mJ, the damage white spot could not be clearly seen. Table 1 showed the copper mode of silica substrate. According the damage of different energy densities of 1064nm laser, it can be basically determined the damage threshold about 5J/cm². Furthermore, the damage threshold is 5J/cm² based on the formula, which shows that the theoretical calculation is consistent with the experimental results.

Table 1. Damage of different energy densities by1064nm

Times	Energy density of laser	Degree of damage
1	100mJ	The damage spot is large and penetrated
2	5mJ	The damage spot is very small but visible
3	2mJ	No damage
4	4mJ	No damage

Table 2. Damage of different energy densities by 532nm

Times	Energy density of laser	Degree of damage
1	50mJ	The damage spot is quite large
2	3mJ	The damage spot is very small but visible
3	2mJ	No damage
4	5mJ	The damage spot is obvious

After the 1064nm laser test was completed, 532nm laser was selected to conduct the experiment with re-calibration operation. When the laser attenuated to 3mJ, the damage was obviously observed on the CCD imaging device. Then, the laser energy density was reduced to 2mJ that no damage spots were found. As shown in Table 2, the estimated critical energy of laser damage is 2~3mJ. Substituted into the formula, the threshold value of 532nm laser damage of copper-plated on silica substrate is 3J/cm². In order to conduct quantitative analysis with 1064nm laser, the laser energy was adjusted back to 5mJ and irradiated near the previous 1064nm

damage spot resulting in a large damaged spot. Therefore, It concluded that the damage threshold of 532nm laser on the sample material is less than that of 1064nm laser. And the damage thresholds of material at two wavelengths were 5mJ/cm² and 3mJ/cm² respectively, which were very close to the measured results 4.6J/cm² and 2.6J/cm² in reference.

3.2 Damage morphology

The damage morphology of different laser wavelength with-1064nm and 532nm was observed which profilometer and electron

microscope were used. The microscope can observe the surface morphology of the laser damage, and the profilometer can observe the contour and depth of the damage, which can be further compared with the subsequent simulation results.

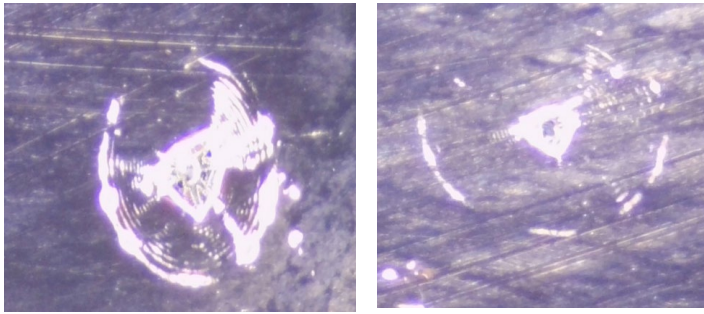


Figure 1: 532nm wavelength damaged surface (left), and 1064nm wavelength damaged surface (right)

As shown in Fig. 1, it can be seen from the microscope that 532nm laser has a larger damage area than 1064nm laser with the same laser energy density. And its reflection degree of light is stronger, the spot shape is more irregular. The reason for this phenomenon is that the wavelength of 532nm is shorter than that of 1064nm, and the photon energy decreases with the increase of wavelength. That is to say, the photon energy of 532nm is stronger than that of 1064nm. Therefore, the surface of the same sample material absorbs the photon energy of short-wavelength more than that of long-wavelength. So, 532nm laser will generate more heat energy than 1064nm on the sample surface during laser damage, which is easier to damage the sample. And the damage area of 532nm will be larger than 1064nm. In addition, the shape of the laser damaged surface is not regular circle but irregular polygon, which is due to impurities in the coating of the sample material, or the interference caused by dust on the surface and the fingerprint, etc.

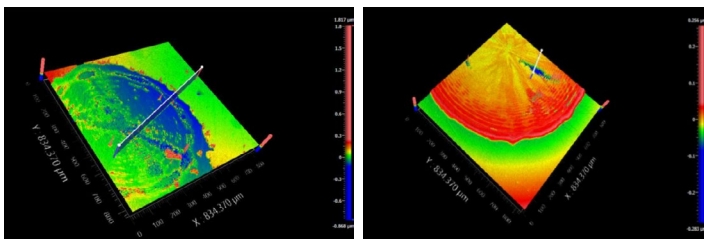


Figure 2: Damage morphology of 532nm laser (left), and 1064nm laser (right)

In addition to observing the surface contour of laser damage, the morphology and depth of laser damage should also be analyzed. The damages caused by the two lasers alone were shown in Fig 2. It can be seen that the damage depth of 532nm from the circumference to the center of the circle is deeper than that of 1064nm at the same position. According to Fig. 3 and 4, the radius of damage pit is about 430μm by 532nm laser and 400μm by 1064nm laser. The depth of the 532nm laser damage pit is about 0.12μm, while the lowest point of the 1064nm laser damage pit is about 0.09μm from

the surface. That is to say, the damage depth of short wave is larger 0.03μm than long wave. In addition, there is the undulating broken lines in the figure. It is considered that caused by: first, the rough coating technology leads to the uneven surface of the sample material; second, the sample surface is stained with dust or fingerprints before the test, which leads to the generation of errors.

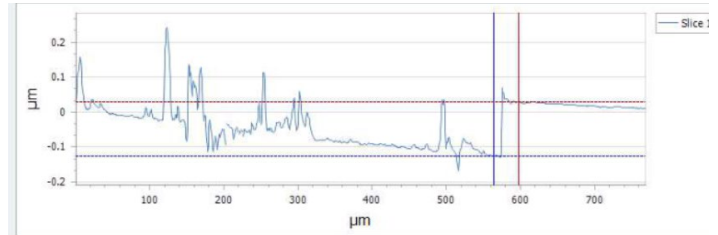


Figure 3: Damage depth curve of 532nm

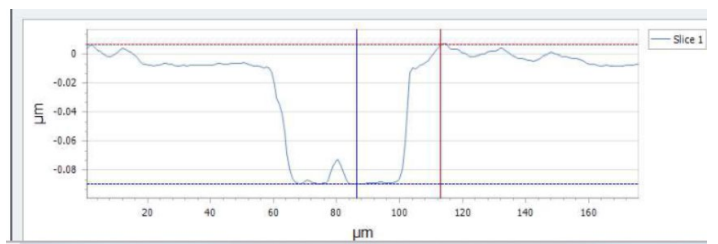


Figure 4: Damage depth curve of 1064nm

The above are the damage morphology of two different laser at 5mJ energy. From the surface damage analysis, we determined that damage area of 532nm laser is larger than 1064nm, and the damage shape is more irregular. For the depth of damage, the short wave is about 0.03μm than the long wave. Meanwhile, the damage morphology obtained is similar to that in reference [3], and the damage area at 532nm is larger. It indicates that 532nm laser has stronger penetration and greater destructive power than 1064nm laser at the same laser energy density.

3.3 Simulation

3.3.1 Parameter setting and model establishment

During the experiment, the two laser beams need to be re-calibrated when switching, which makes it difficult to act on the same point together. Therefore, in order to study the effect of 1064nm and 532nm laser beams together and the difference in the total energy ratio between them to test the damage degree during the joint action, COMSOL was used to simulate dual-wavelength laser damage. The model was established and parameters were set to simulate the temperature field distribution of explosive bridge damage under two different wavelengths with different proportions and judge the primary and secondary induced conditions. As shown in Table 3 and 4, the parameters module were defined including the heating heat, specific heat capacity, thermal conductivity, and the burning temperature of the material. The position of the laser damage, the total power, laser frequency and laser radius of the 1064nm and 532nm laser, respectively, are provided. The average power of the laser was calculated by using the formula:

$$P_0 = P / (\pi * R^2 * H),$$

in which P is the laser power, R is the spot radius, and H is the frequency.

Table 3. Parameters of 1064nm laser and material

Symbolic	Expression	Value	Parameter Name
H _s	560[kJ/kg]	5.6E5 J/kg	Sublimation heat
T _a	675[degC]	948.15 K	Burning temperature
rho	8900[kg/m ³]	8900kg/m ³	Density
Cp	900[J/kg/K]	900 J/(kg•K)	Specific heat
k	231[W/m/K]	231 W/(m•K)	Coefficient of thermal conductivity
r _{sport}	100[μm]	1E-4 m	Spot radius
x0	5800[μm]	0.0058 m	Left spot position
x1	6200[μm]	0.0062 m	Right spot position
P _{total}	6[W]	6 W	Total laser power
P _{density_avg}	P _{total} /(pi*r _{sport} ² *H)	5.57W/cm ²	Average laser power density
H	15000	15000	Laser frequency

Table 4. Parameters of 532nm laser and material

Symbolic	Expression	Value	Parameter Name
H _s	560[kJ/kg]	5.6E5 J/kg	Sublimation heat
T _a	675[degC]	948.15 K	Burning temperature
rho	8900[kg/m ³]	8900kg/m ³	Density
Cp	900[J/kg/K]	900 J/(kg•K)	Specific heat
k	231[W/m/K]	231 W/(m•K)	Coefficient of thermal conductivity
r _{sport}	100[μm]	1E-4 m	Spot radius
x0	5800[μm]	0.0058 m	Left spot position
x1	6200[μm]	0.0062 m	Right spot position
P _{total}	6[W]	6 W	Total laser power
P _{density_avg}	P _{total} /(pi*r _{sport} ² *H)	2.82W/cm ²	Average laser power density
H	20000	20000	Laser frequency

Then, the material model was set. Because it is a coating double-layer structure, so the setting is stratified. The overall structure is rectangular, the upper layer is copper about 1000μm thick, and the lower layer is silica set 9000μm thick. Thus the total thickness is 10000μm, which the total length is 12000μm, and the width is 10000μm. To further set up solid heat transfer, two heat flux modules are required. So convective heat flux was selected on the upper surface: $q_0 = h(T_{ext} - T)$, where heat transfer coefficient was: $h = h_a ((T - T_a) [1/K])$, in which h_a is a slope function, T is temperature, T_a is heat of ascension, and K is thermal conductivity constant. The lower surface selected the generalized inward transfer heat flux, where q_0 refers to the above equation. Finally, two free triangle networks are added, the geometric entities are set as domains that the upper and lower layers of the material are selected respectively. As the damage of thin film is mainly studied, the upper mesh is set as extremely fine, while the lower layer is set as normal. The final structure is shown in Fig. 5.

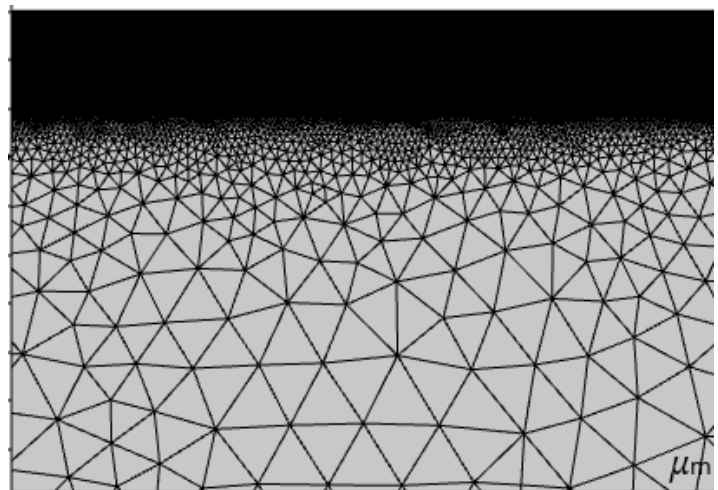


Figure 5: Mesh division of geometric structure

To establish the dual-wavelength model on the basis of the single-wavelength, a new frequency H_2 and laser energy P_{total_2} should be added into the parameters. And the average laser power should be calculated, as shown in Table 5. The analytical function is set as the sum of the two laser beams: 1064nm laser power \times Gaussian pulse \times piecewise function + 532nm laser power \times Gaussian pulse

\times piecewise function. After setting, calculation was carried out to analyze the effect of single wavelength and multi-wavelength. Furthermore, the distribution of laser damage temperature field and the primary or secondary induced conditions of each pulse.

Table 5. The Parameters of the two Wavelengths of Lasers Work Together

Symbolic	Expression	Value	Parameter Name
H_s	560[kJ/kg]	5.6E5 J/kg	Sublimation heat
T_a	675[degC]	948.15 K	Burning temperature
rho	8900[kg/m^3]	8900 kg/m ³	Density
Cp	900[J/kg/K]	900 J/(kg•K)	Specific heat
k	231[W/m/K]	231 W/(m•K)	Coefficient of thermal conductivity
r_sport	100[μm]	1E-4 m	Spot radius
x ₀	5800[μm]	0.0058 m	Left spot position
x ₁	6200[μm]	0.0062 m	Right spot position
P_total	4.2[W]	4.2 W	532nm Total laser power
P_total2	1.8[W]	1.8W	1064nmTotal laser power
P_density_avg	$P_{total}/(\pi \cdot r_{sport}^2 \cdot H)$	6684.5W/m ²	532nmAverage laser power density
P_density_avg2	$P_{total2}/(\pi \cdot r_{sport}^2 \cdot H2)$	3819.7W/m ²	1064nmAverage laser power density
H ₁	20000	20000	532nm Laser frequency
H ₂	15000	15000	1064nm Laser frequency

3.3.2 Analysis of simulation results

When 532nm laser parameters were put into the model, the evolution curve of the damage depth by single-wavelength over time was obtained, as shown in Fig. 6. In order to compare the damage of different laser at the same time, the results were selected at 1μs. It can be seen from the figure that the etching depth of 532nm laser alone is about 0.10μm at 1μs, which is smaller than the experimental damage depth. The reason may be that the simulation is carried

out under ideal conditions. While the material is doped with other impurities or contaminated in the experimental process, which affects the damage threshold and leads to greater damage degree. Then,1064nm laser is applied at a single wavelength, resulting in a depth of about 0.072μm at 1μs, as shown in Fig 7. It is shallower than the experimental ablation depth of 0.09μm, which is caused by the material itself and human factors as mentioned above.

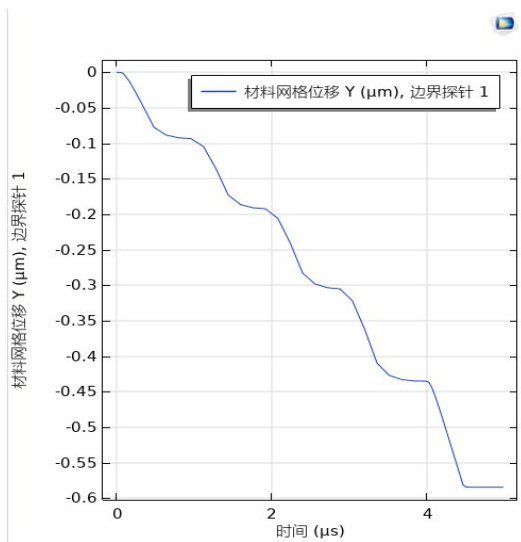


Figure 6: The ablation depth of 532nm laser alone

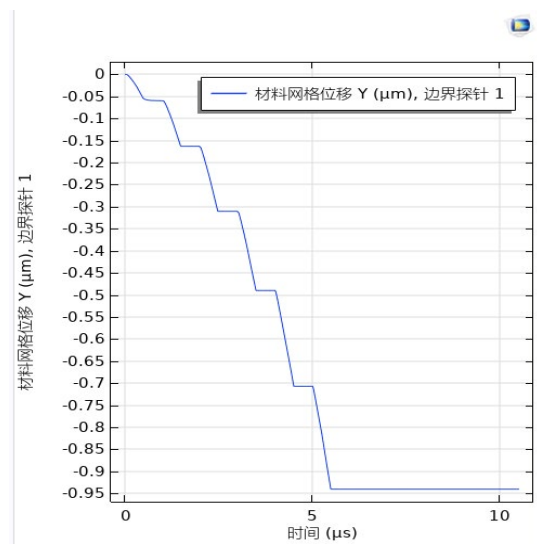


Figure 7: The ablation depth of 1064nm laser alone

By changing the ratio of 1064nm and 532nm laser to the total energy density and the degree of material damage, the primary and secondary factors of the two laser-induced explosive bridges were determined. The same energy density and action time of 1064nm and 532nm in the model were used to compare the damage depth at different proportions. Since the experimental results showed that 532nm laser has a larger damage surface area and deeper damage depth than 1064nm laser, it is assumed that 532nm laser plays a dominant role in the damage process. When the energy density ratio of 1064nm and 532nm was selected as 3:7, the damage depth and temperature field distribution were calculated according to the model, as shown in Fig. 8. It can be seen that the slope of the dam-

age depth curve from the surface to the interior of bridge film is between the two pulses alone, and the highest temperature at the damage center up to 950K. In this temperature field, the energy in the spot center is the highest and decays to both sides. So the ablation temperature in the center is the higher than the two sides. As a whole, the damage depth presents a gradient distribution with the depth what the reason is that the model is built in the form of piecewise function, so that the change of laser damage effect with time can be seen more obviously. In addition, the damage depth of the two kinds of laser dominated by 532nm is 0.099 μm at 1 μs , which is close to the depth of 0.10 μm by 532nm alone.

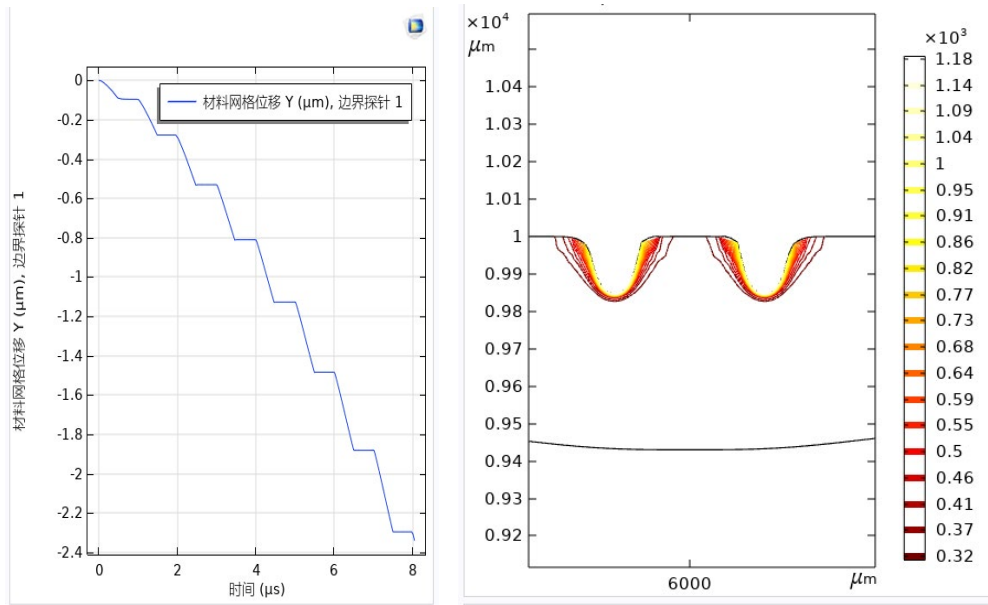


Figure 8: Damage depth (left) and temperature field distribution (right) when 532nm laser energy is dominant

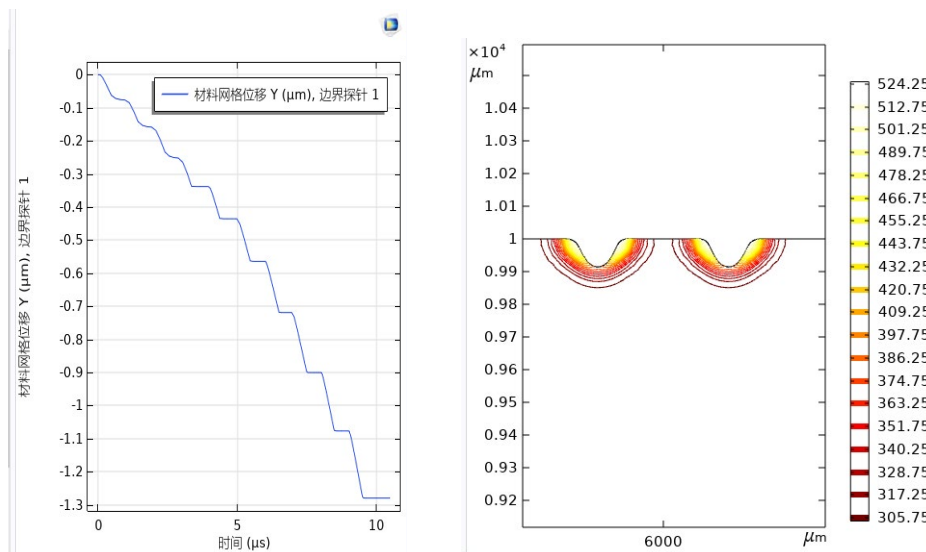


Figure 9: Damage depth (left) and temperature field distribution (right) when 1064nm laser energy is dominant

Meanwhile, when 1064nm and 532nm lasers accounted for 7:3 of the total energy density, the temperature field distribution and damage depth were obtained, as shown in Fig 9. It can be seen that the maximum temperature in the center of the field is 489K. And the depth of damage pit is shallower than that of 532nm laser. But the damage depth of 1064nm laser with double pulse is deeper than that of 1064nm laser alone, which is caused by the addition of 532nm laser energy. At 1 μ s, the damage depth of the dual laser had increased 14% compared with that of the 1064nm laser alone, and the percentage increases with time. Therefore, by comparing the different proportions of the two energy densities, it is concluded that the damage depth is deeper when the 532nm laser energy takes up more of the total energy than the 1064nm laser in the same time, and this effect becomes more obvious with time delay. When the same laser duration is 8 μ s, the damage depth of 532nm laser is 2.3 μ m, while the damage depth of 1064nm laser is 1.30 μ m. Therefore, the laser damage depth is deeper by dominant 532nm, and the damage effect is more obvious in the same time. In this way, the energy ratio of multiple laser beams can be adjusted to meet the requirements of different conditions with laser processing or explosive foil ignition.

4. Conclusion

In this paper, the influence of different laser pulses on the damage of explosive bridge was studied. The damage morphology and threshold value were obtained by laser damage experiment and theoretical calculation with copper plating on silicon dioxide. On this basis, the temperature field distribution of primary and secondary induced and explosive bridge damage under different pulse energy ratio was simulated. The density, internal stress and hardness of thin films are different due to different materials, resulting in different laser damage thresholds. Because the hardness of silicon dioxide is stronger than that of silicon and its density is larger. So the internal stress of silicon dioxide is stronger than that of silicon. Therefore, the damage threshold of silicon is smaller than that of silicon dioxide after laser damage after passing through the coating. By different lasers, it is concluded that the factors affecting the damage threshold included laser wavelength, density and hardness of the sample material, etc. When the two wavelengths alone to damage the explosive bridge, we concluded that the shorter the wavelength, the more obvious the damage effect and the lower the damage threshold by analysis the damage area, shape and depth.

COMSOL was used to simulate the joint action of 1064nm and 532nm lasers to damage in different proportions. The results show that when the laser duration is 8 μ s, the damage depth of 532nm laser is 2.3 μ m, while that of 1064nm is 1.30 μ m. It indicates that 532nm laser is more likely to cause damage to explosive bridge materials than 1064nm, and the effect is more obvious. The 532nm laser is the main inducement, which is also consistent with the results of literature. Therefore, this study is beneficial to better understanding the laser damage and processing technology improvement of explosive bridge. And it also can realize the synchronization and high efficiency of the ignition of the energy converter devices.

Acknowledgment

Financial support was obtained from the National Natural Science Foundation of China (No: 11947126, 62001363), National Defense Pre-Research Foundation of China (No: 6140619010301,

61406190501), Science and Technology Department of Shaanxi Province (No: 2022JQ-027), Education Department of Shaanxi Province (No: 20JK0689), and Science Project of Beilin District (No: GX2138).

References

1. Ni Xiaowu, Lu Jian, He Anzhi, Wang Pingqiu, Ma Zi, et al. (1994) *Laser Technology*, 06: 348-352.
2. Sun Guorong (2009) Study on the effect of short pulse laser irradiation on semiconductor Si irradiation. *Harbin Institute of Technology*, 4- 99-102.
3. Zhou Ming, Zhao Yuan-An, Li Dawei, Fan Zhenxiu, Shao Jinda (2009) Damage of thin films irradiated by 1064nm and 532nm lasers. *Chinese journal of lasers*, 36: 3050-3054.
4. RW Eloppe and DR uhlmann (1970) Mechanism of inclusion damage in laser glass. *Jour of Appl Phys*, 41: 4023-4037.
5. M Sparks, CT Duthler (1973) Theory of infrared absorption and material failure in crystal containing inclusion. *J. Appl. Phys*, 44: 3038-3045.
6. Thomas W Walker, Athur H Guenther, Philip E Nelsen (1981) Pulsed laser-induced damage to thin film optical coating-part I: Experimental and part II: Theory. *IEEE Journal of quantum Electronics*, 17: 2041-2052.
7. Bonneau F, Combis P, Rullier Jet al. (2002) Study of UV laser interaction with gold nanopartical sembedded in silica. *Appl Phys B*, 75: 803-815.
8. M Mansuripur, GA Neville Connell, J W Goodman (1982) Laser-induced local heating of multilayers. *Applied Optics*, 21: 1106-1114.
9. Zhao Qiang, Fan Zhengxiu (1996) Effect of interfacial absorption on temperature field of optical thin film. *Acta Optica Sinica*, 06: 777-782.
10. Zhao Qiang, Fan Zhengxiu, Wang Zhijiang (1999) Numerical analysis of laser heating process of optical thin films. *Acta Optica Sinica*, 08: 1019-1023.
11. Tan Hengying, Liu Pengcheng, Shi Baixuan (2005) Nondestructive Detection of Laser Damage in optical thin films by laser photothermal deflection imaging. *Acta Photonica Sinica* 01: 158-160.
12. Rongbing Gan, Libin Lin, Xiaodong Jiang, Zuxin Huang, Wei Zhong, et al. (2002) High Power Laser and Particle Beams, 01: 45-48.
13. Cui Yun, Zhao Yuanan, Jin Yunxia, Zhang Weili, Qi Hongji, et al. (2006) *Journal of Vacuum Science and Technology*, 04: 321-325.
14. Sun Chengwei, Lu Qisheng, Fan Zhengxiu (2002) Laser irradiation effect. Beijing: National Defense Industry Press, 08: 280-287.
15. E Hacker, H Lauth (1996) Review of structural influences on the laser damage threshold of oxide coatings, 27: 316-330.

Copyright: ©2022 Shenjiang Wu, et al. This is an open-access article distributed under the terms of the Creative Commons Attribution License, which permits unrestricted use, distribution, and reproduction in any medium, provided the original author and source are credited.